The Typically Disordered N-Terminus of PKA Can Fold as a Helix and Project the Myristoylation Site into Solution‡

Christine Breitenlechner,*,⊥ Richard A. Engh,*,⊥,# Robert Huber,⊥ Volker Kinzel,§ Dirk Bossemeyer,§ and Michael Gassel§,||

Abteilung Strukturforschung, Max-Planck-Institut fuer Biochemie, 82152 Martinsried, Germany, Department of Pathochemistry, German Cancer Research Center, 69120 Heidelberg, Germany, and Department of Medicinal Chemistry, Roche Diagnostics GmbH, 82372 Penzberg, Germany

Received December 16, 2003; Revised Manuscript Received March 9, 2004

ABSTRACT: Protein kinases comprise the major enzyme family critically involved in signal transduction pathways; posttranslational modifications affect their regulation and determine signaling states. The prototype protein kinase A (PKA) possesses an N-terminal α-helix (Helix A) that is atypical for kinases and is thus a major distinguishing feature of PKA. Its physiological function may involve myristoylation at the N-terminus and modulation via phosphorylation at serine 10. Here we describe an unusual structure of an unmyristoylated PKA, unphosphorylated at serine 10, with a completely ordered N-terminus. Using standard conditions (e.g., PKI 5−24, ATP site ligand, MEGA-8), a novel 2-fold phosphorylated PKA variant showed the ordered N-terminus in a new crystal packing arrangement. Thus, the critical factor for structuring the N-terminus is apparently the absence of phosphorylation of Ser10. The flexibility of the N-terminus, its myristoylation, and the conformational dependence on the phosphorylation state are consistent with a functional role for myristoylation.

Protein kinases are a centrally important enzyme family involved in signal transduction pathways. The principal signaling mechanisms are phosphorylation and dephosphorylation events that can switch protein kinases between active and inactive states, often accompanied by secondary structure rearrangements. Inactivity is associated most often with displacements of helix C, the major alpha helix of the kinase domain N-lobe, with concomitant disruption of an active site salt bridge. This conserved element consists of a lysine residue that is often mutated in "kinase dead" variants and a glutamate residue centrally anchored in helix C. Other inactivating conformations involve the activation loop, often by blocking the active site or by locking helix C into an inactive conformation. In more than half of all protein kinase structures, inactivity is associated with a sterical block in the ATP-binding site (*1*−*3*).

These mechanisms of regulation are rapid and allow the cell to react swiftly and reliably to external and internal stimuli. When protein regulation fails, underactivity and especially overactivity can cause disease, such as cancer with its characteristic deregulation of signals controlling proliferation, apoptosis, adhesion, and/or invasion. Thus, protein activity requires strict control and high signal transduction fidelity for proper physiological function. With more than 500 protein kinases in the human genome, and a wide variety of control mechanisms in addition to conformational changes at the catalytic site, many or most kinase specific control mechanisms have not yet been fully characterized or even identified. These mechanisms include substrate and cofactor docking sites, control of expression levels, and cellular location, among others. For PKA, the subcellular distribution of the PKA catalytic subunit is governed by regulatory subunits and anchoring proteins (*4*−*8*), including the translocation of PKA between the cytoplasm and the cell nucleus (*9*−*11*). Despite extensive studies of PKA over the past decade, many fundamental aspects of these control mechanisms remain unclear.

The N-terminus of PKA is characterized by a 30−40 residue segment that contains an alpha helix denoted helix A. This feature is unique to PKA and distinguishes it also from its fellow subgroup AGC kinases. The N-terminal segment begins with the sequence GNAAAAKKGSEQESV and undergoes several posttranslational modifications (*12*): myristoylation of Gly1, deamidation of Asn2, and phosphorylation of Ser10. PKA isolated from mammalian tissues differs from recombinant enzyme expressed in *Escherichia coli.* Protein from eukaryotic cells is myristoylated at Gly1, whereas recombinant protein is not, unless coexpressed with myristoyltransferase (*13*). Deamidated Asn2 is found in 30% of PKA isolated from muscle tissue, but not in recombinantly

‡ The coordinates have been deposited in the Protein Data Bank (PDB) with the accession number 1SMH.

* To whom correspondence should be addressed. E-mail: breitenl@biochem.mpg.de, engh@biochem.mpg.de; phone 0049-89-85782630; fax 0049-89-85783516.

⊥ Max-Planck-Institut fuer Biochemie.

§ German Cancer Research Center.

Roche Diagnostics GmbH.

|| Current address. Drug Discovery, Intervet Innovation GmbH, 55270 Schwabenheim, Germany.

[1] Abbreviations: PKA, protein kinase A; PKAB2, PKA mutant with amino acid exchanges Val123Ala and Leu173Met; PKAB3, PKA mutant with amino acid exchanges Val123Ala, Leu173Met, and Gln181Lys; PKAB4, PKA mutant with amino acid exchanges Gln84Glu, Val123Ala, Leu173Met, and Phe187Leu; 2P-PKAB4, 2-fold phosphorylated mutant PKAB4 (pThr197, pSer338); 3P-PKA, 3-fold phosphorylated PKA (pSer10, pThr197, pSer338); 2P-myrPKA, 2-fold phosphorylated and N-terminal myristoylated PKA (pThr197, pSer338).

10.1021/bi0362525 CCC: $27.50
Published on Web 05/29/2004

expressed enzyme (*14*). Ser10 is known as an autophosphorylation site in vitro (*15*, *16*). A functional role has not been described yet. Ser10 phosphorylated PKA has not been isolated from mammalian tissues, thus indicating a transient phosphorylation (*17*). Recombinant PKA from *E. coli* is often phosphorylated at this site, depending on the time of induction of expression.

For several myristoylated proteins, changes in the electric charge are part of the so-called myristoyl electrostatic switch mechanism for the modulation of enzyme translocation and membrane interaction (*18*−*20*). Myristoylation of Src kinase is associated with membrane binding, and chimeric PKA-Src constructs showed that myristoylated N-terminal sequences of PKA fused to Src kinase can also bind to membranes (*21*). Like Src, PKA can be released from membranes upon platelet-derived growth factor stimulation in fibroblasts (*18*, *22*). Further, myristoylated 14-residue N-terminal PKA peptides interact with phospholipid bicelles (*23*). In addition to the myristoylation site, basic residues (Lys7 and Lys8) of the N-terminal sequence also conform to typical membrane binding features. The myristoylated catalytic subunit can bind to liposomes in vitro as shown with fluorescence resonance energy transfer (FRET) methods. Myristoylation and complex formation with regulatory subunit RII (but not RI) enhance liposome binding synergistically (*24*). Myristoylation of the N-terminus also stabilizes the enzyme fold via binding of the myristoyl chain in a hydrophobic pocket of the C-lobe (*25*).

Several conformations of the N-terminus have been observed in different crystal structures. Usually, however, it is disordered for the first 11−14 residues followed by alpha helix A (*25*−*27*); the helix is often observed also beginning with residue Ser10 when phosphorylated. The addition of detergent MEGA-8 to crystallization trials may influence the extent of helix A formation by mimicking myristoyl binding.

PKA isolated from mammalian organs such as heart are found phosphorylated at Thr197 of the activation loop and Ser338 of the C-terminus, the two phosphorylation positions that are known to be activating and important for catalysis and often have equivalent functions in cognate kinases. In contrast, Ser10 was identified as an in vitro autophosphorylation site (*15*). Expressed in *E. coli*, PKA is heterogeneously phosphorylated at Ser10 and Ser139, in addition to uniform phosphorylation at the sites Thr197 and Ser338 (*16*). All isoforms are catalytically equivalent to mammalian protein (*28*). A structural function can be attributed to pThr197, tightly bound via polar interactions near the catalytic site. pSer338 is important for stability as it anchors the C-terminus on the small lobe (*16*). Structural roles for the other sites are less clear. They are variously more flexible than Thr197, as shown by crystal structures and also by ^{31}P NMR spectroscopy (*29*). In contrast to the other phosphorylation sites, phosphorylated Ser10 is especially flexible or disordered.

Tholey et al. studied the influence of these posttranslational modifications on the structural behavior of the N-terminus of PKA using circular dichroism (*12*) and showed their importance for fine-tuning of enzyme assembly and function. Phosphorylation of Ser10 decreases the extent of folding, whereas myristoylation seems to have a structuring effect. Deamidation of Asn2 seems to be uncorrelated with structural changes, but may affect membrane binding affinity due to the introduction of a negative charge.

Table 1: Expression Pattern of Multiple Phosphorylated Forms of PKA Wild-Type and the PKAB4 Mutant

	peak 1 (4P-PKA) (%)	peak 2 (3P-PKA) (%)	peak 3 (2P-PKA) (%)
PKA	41	51	8
PKAB4	10	34	56

Peak 1 is 4-fold phosphorylated (Ser10, Ser139, Thr197, and Ser338), peak 2 is 3-fold phosphorylated (Ser10, Thr197, and Ser338), and peak 3 is 2-fold phosphorylated (Thr197 and Ser338)

Here we describe the first PKA structure with a completely ordered N-terminus, clearly defined in the electron density with helix A starting at Gly1. The protein is not myristoylated; MEGA-8 (N-Octanoyl-N-methylglucamine) was present in the crystallization experiment and electron density for the octanoyl moiety can be found in a position normally occupied by myristate. Further, the protein is not phosphorylated at Ser10. This combination apparently leads to the extension of the α-helix to the N-terminus in the isolated protein, a conformation that projects an exposed myristoylation site away from the protein.

MATERIAL AND METHODS

Mutagenesis of PKA. Site-directed mutagenesis was performed using pT7-PKA as template and the Stratagene (La Jolla) Quick Change kit following the manual of the supplier including the design of the corresponding primer pairs. All constructs used for protein expression were verified by DNA sequencing. The PKAB2 (Val123Ala/Leu173Met) and PKAB3 (Val123Ala/Leu173Met/Gln181Lys) mutants have been described previously (*30*). The PKAB4 mutant has four amino acid exchanges at the ATP binding site. They are, compared to wild-type protein, Gln84Glu, Val123Ala, Leu173Met, and Phe187Leu.

Expression and Purification. Expression vectors pT7-7 and pET28b, both carrying a T7-promoter, were used to express bovine PKA Cα and PKAB4 in *E. coli* strain BL21 (DE3), respectively. Two positions distinguish bovine (Asn32, Met63) from human PKA (Ser32, Lys63). The mutant protein PKAB4 was expressed and purified via affinity chromatography and ion exchange chromatography as established for PKA and described previously (*27*, *30*, *31*). In comparison to wild-type protein, the expression yield of the PKAB4 mutant is reduced. The pattern of the different phosphorylated forms has changed and the predominant fraction was 2-fold phosphorylated (Table 1). Thus, 2-fold phosphorylated PKAB4 was used for crystallization trials.

The identity of the sample and phosphorylation state was confirmed by the total mass of the protein determined by ESI mass spectrometry. For LC-MS, the microgradient system type 140c (Perkin-Elmer) coupled to PE SCIEX API 165 ESI detector was used with a Nucleosil C_8 100-5 column and a linear gradient of 20−95% acetonitrile in water with 0.1% TFA in 15 min. The spectra were deconvoluted with the BioMultiview 1.4 software.

Activity Tests. The determination of enzyme activity was accomplished by an ATP regenerative, NADH consuming assay according to Cook (*32*). The assay mix (100 mM

Table 2: Data Collection and Refinement Statistics

Data Collection	
Beamline	BW6 DESY Hamburg
wavelength (Å)	1.0500
space group	$P2_12_12_1$
cell (a, b, c) (Å)	48.8, 79.4, 117.8
resolution range (Å)	48−2.044
no. of unique reflections	29196
completeness (%) [last shell 2.04−2.15]	98.1 [91.9]
I/σ (I) [last shell 2.04−2.15]	6.1 [1.9]
average redundancy [last shell 2.04−2.15]	4.4 [4.0]
R_{sym} [last shell 2.04−2.15]	0.089 [0.365]
Refinement	
R-factor (%)/free R-factor (%)	18.9/23.8
free R-value test size (%)	5.1
correlation coefficient $F_o - F_c$ [free]	95.0 [92.2]
Standard Deviation from Ideal Values	
bond length (Å)	0.015
bond angles (°)	1.428
Temperature Factors	
all atoms	28.4

MOPS pH 6.8, 100 mM KCl, 10 mM $MgCl_2$; 1 mM phosphoenolpyruvate, 0.1 mM Kemptide, 1 mM β-mercaptoethanol, 15 units/mL lactate-dehydrogenase (Sigma); 8 units/mL pyruvate kinase (Sigma), 0.21 mM NADH) was completed by the addition of enzyme and the reaction was started with ATP. The time-dependent decrease of NADH was measured at 340 nm with three independent measurements per data point.

X-ray Crystallography. Hanging drops containing 18 mg/mL protein, 25 mM Mes-BisTris pH 6.4, 75 mM LiCl, 1.5 mM octanoyl-*N*-methylglucamide, 1 mM PKI(5−24) were equilibrated at 5 °C against 12−18% methanol. One crystal was sufficient to obtain a complete data set. Diffraction data of the flash-frozen PKAB4 crystals were measured at the synchrotron beamline BW6 at the DESY (Hamburg, Germany). (*R,R*)-(−)-2,3-butanediol was used as cryoprotectant. The data were processed with the program MOSFLM and SCALA. The crystal has the orthorhombic symmetry $P2_12_12_1$ with cell constants $a = 48.8$, $b = 79.4$, $c = 117.8$. The structures were determined by molecular replacement using AMoRe from the CCP4 program package (www.ccp4.ac.uk/main/html) (*33*, *34*). As starting model, we chose a PKA structure in a closed conformation (to be published). Refmac 5.1.24 was used for refinement, while MOLOC (www.moloc.ch) (*35*) was used for graphical evaluation and model building. For data reduction and refinement statistics, see Table 2. The structures are depicted in Figures 1 and 2 with graphics from the programs MOLSCRIPT (*36*), BOBSCRIPT (*37*), and Raster3d (*38*).

RESULTS

Overall Structure. The structure we describe here is a complex of several components. The pseudosubstrate peptide PKI(5−24), the detergent MEGA-8, and a low molecular weight ATP competitive inhibitor are bound to a 2-fold phosphorylated active site mutant of PKA (Gln84Glu, Val123Ala, Leu173Met, and Phe187Leu compared to wild-type, here termed 2P-PKAB4). Although the complex was crystallized under previously established conditions and generated the typical orthorhombic space group ($P2_12_12_1$), a new crystal packing arrangement was formed. The crystal diffracted to 2.05 Å resolution. In this crystal, PKAB4 adopts a closed conformation, and all 350 residues are ordered and resolved, most notably beginning with the first residue (Gly1). This is in contrast to most structures, in which the N-terminus is typically disordered for the first 10−15 residues (Figure 1). The electron density confirms phosphorylation at the two sites Thr197 and Ser338, and shows the ordering of the octanoyl moiety of MEGA-8 in the myristate binding pocket. In this manuscript, we analyze the influence of phosphorylation and myristoylation on the conformation of the N-terminal Helix A.

Phosphorylation State. This active site mutant PKAB4 (with mutations Gln84Glu, Val123Ala, Leu173Met, and Phe187Leu) binds ATP 12 times more weakly than does wild-type PKA (Table 3). As previously described for the PKAB2 mutant (Val123Ala and Leu173Met) (*30*), this is explained by a conformational transition of Gln181 that can occur in combination with mutations Val123Ala and Leu173Met. The expression yield of PKAB4 in *E. coli* is reduced compared to wild-type, and autophosphorylation is also less extensive (Table 1). Therefore, the doubly phosphorylated protein was used for crystallization (verified by mass spectroscopy). The crystal structure with all residues resolved shows Thr197 and Ser338 are phosphorylated, whereas Ser10 and Ser139 are clearly unphosphorylated.

Effects of Myristoylation on Crystallization. Protein extracted from tissues is myristoylated at Gly1, whereas recombinant protein from *E. coli* is not, unless coexpressed with myristoyltransferase (*13*). Crystal structures from recombinant protein lacking myristate are resolved beginning at residues Gln12 or Val15 sometimes even beginning at Ser10 or Lys7 as in case of 1Q8U (*39*). MEGA-8 in the solution mimics in part myristate binding and seems to stabilize the helix; the octanoyl part of MEGA-8 is also resolved (1APM, 1Q61, 1Q8U, and others) (*30*, *39*, *40*). Under these conditions, high B-factors for phosphorylated Ser10 indicate considerable flexibility despite the increased ordering. ^{31}P NMR spectroscopy also shows high flexibility in comparison with the other phosphorylation sites (*29*).

The 3- and 4-fold phosphorylated PKA preparations crystallize most readily, but in the case of the PKAB4 mutant we attempted crystallization using the 2-fold phosphorylated protein. Crystallization success led to the first structure with a completely ordered N-terminus. Of the three myristoylated PKA structures available in the protein data bank (1CDK, 1CMK, 1CTP) (*25*, *41*), all show disorder at the N-terminus, but 1CMK includes model coordinates for the entire N-terminus: localization of the myristoyl chain in the 2.9 Å structure (Figure 2) requires non-helical geometry at the N-terminus to enable myristoyl binding in a pocket made up by residues from Helix A (explicitly, Val15, Phe18, and Leu19), Phe100, Helix E (explicitly, Leu152, Glu155, Tyr156), and Helix J (explicitly Asp301, Ile303 and Tyr306) residues. The 2.0 Å structure of myristoylated PKA from heart muscle tissue (1CDK) showed similar features but may have been more disordered at the N-terminus.

One structure (1L3R) has been reported in which the first four amino acids (without side chains) were resolved bound to a pocket formed by other residues, explicitly, Gln181, Leu103, Phe100, Arg308, Tyr306 followed by a disordered region till residue 14 where helix A starts. The protein used for crystallization was 4-fold phosphorylated (Ser10, Ser139,

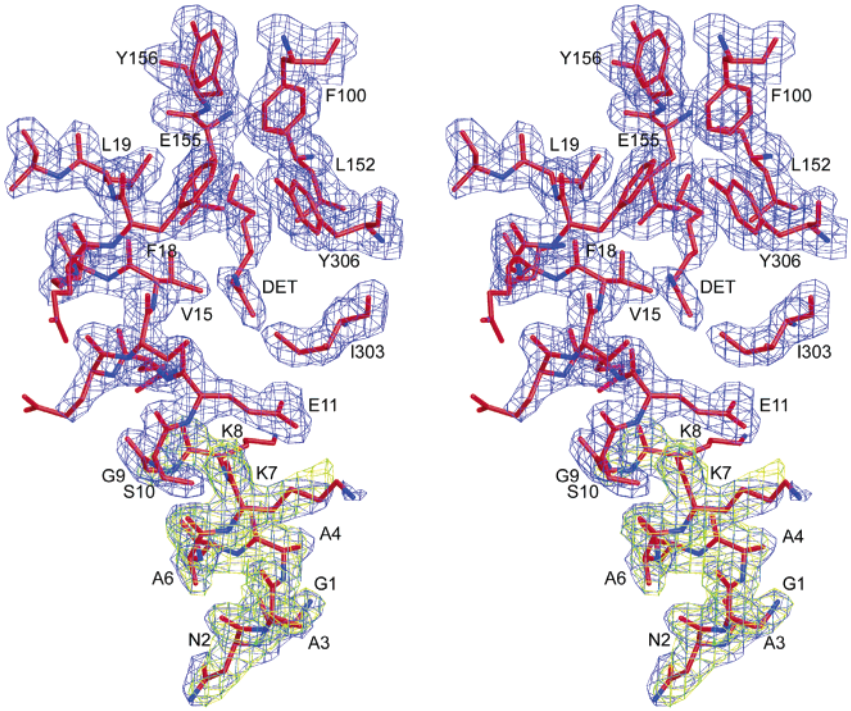

FIGURE 1: The completely resolved N-terminal helix A with the refined $2F_o - F_c$ map (blue) and an $F_o - F_c$ omit map (green) prior to building residues 1−9 (contoured at 1σ and 2σ, respectively). Helix A is clearly defined in the electron density beginning with the first residue Gly1; several solvent-exposed side chains are disordered or show multiple conformations. As the protein was expressed in *E. coli* it is not myristoylated at Gly1. However, the detergent MEGA-8 (*N*-octanoyl-glucamine) occupies the position of the myristoyl chain.

Ser338, Thr197), nonmyristoylated, recombinant mouse PKA (*42*).

Effects of Phosphorylation. Figure 1 shows the N-terminal helix with a refined $2F_o - F_c$ map and a $F_o - F_c$ map prior to building residues 1−9. Helix A is clearly defined in the electron density beginning with the N-terminal residue Gly1. Several solvent-exposed side chains are disordered or show multiple conformations. These results are in good agreement with peptide experiments: Tholey and co-workers have shown that phosphorylation destabilizes the turn and helix structure of peptides designed based on the PKA N-terminal sequence. Further, myristoylation promotes a helical structure (*12*). These findings are in good agreement with our structures, as most structures of 3- and 4-fold phosphorylated PKA (including Ser10 phosphorylation) are disordered at the N-terminus.

The superposition of Figure 2 shows representative structures of the different orientations observed for helix A. In the myristoylated structure (1CMK), Ser10 is unphosphorylated. Helix A begins after a segment that is folded such that the peptide chain lies antiparallel to the helix and brings the myristoyl chain to a hydrophobic pocket. In the PKAB4 structure, this pocket is occupied by the ordered octanoyl moiety of detergent MEGA-8. In the complex of PKA, PKI, and H-1152P (1Q8U, (*39*)) the first 6 N-terminal residues are not visible and the ordered part begins at Lys7-folded as a turn but stretches into another direction compared to PKAB4 and 1CMK; the phosphate group at Ser10 is well defined. Helix A begins with residue pSer10. The Ser10 phosphorylation thus seems to cause the disordering of the N-terminus in unmyristoylated PKA.

Crystal Contacts. We observed a new crystal packing arrangement in the $P2_12_12_1$ spacegroup, with new cell constants. We find several crystal contacts from N-terminal residues Gly1, Asn2, Ala3, Ala4, Ala6, and Lys7 to symmetry-related molecule residues Ile210, Leu211, Ser212 (Helix E1) and Ile244, Tyr247, Glu248, Val251 (Helix G). The N-terminal amino group forms a salt bridge with Glu248.

DISCUSSION

The structure reported here differs from mammalian PKA isolate structures by its lack of N-terminal myristoylation, and differs from recombinant PKA structures by its lack of phosphorylation at serine 10. Additionally, the protein is a 4-fold mutant of PKA, and crystallizes in a new crystal packing arrangement. With this structure, we observe for the first time a completely ordered N-terminus for PKA. The cause—dephosphorylation, unmyristoylation, or crystal packing—of the helical fold of the N-terminus is not immediately apparent. Comparison with existing crystal structures however supports the conclusion that the combined lack of both Ser10 phosphorylation and N-terminal myristoylation stabilizes the extended helical structure sufficiently for crystallization.

The primary effect of the 4-fold mutation was to lower its activity and enhance the relative yield of 2-fold phosphorylated protein (Table 1). The mutations are inside the ATP pocket, distant from the N-terminus, cause no significant structural changes, and do not have contacts to symmetry-related molecules or the N-terminus. Observation of other 3- and 4-fold phosphorylated PKA mutants in the typical packing arrangement confirms that the mutations do not force a crystal packing change. Since unmyristoylated N-termini are typical for recombinant PKA structures, the lack of myristoylation also does not induce the new crystal packing arrangement. The lack of Ser10 phosphorylation removes a crystal contact that exists in other recombinant PKA crystal structures (typically from the phosphate to a

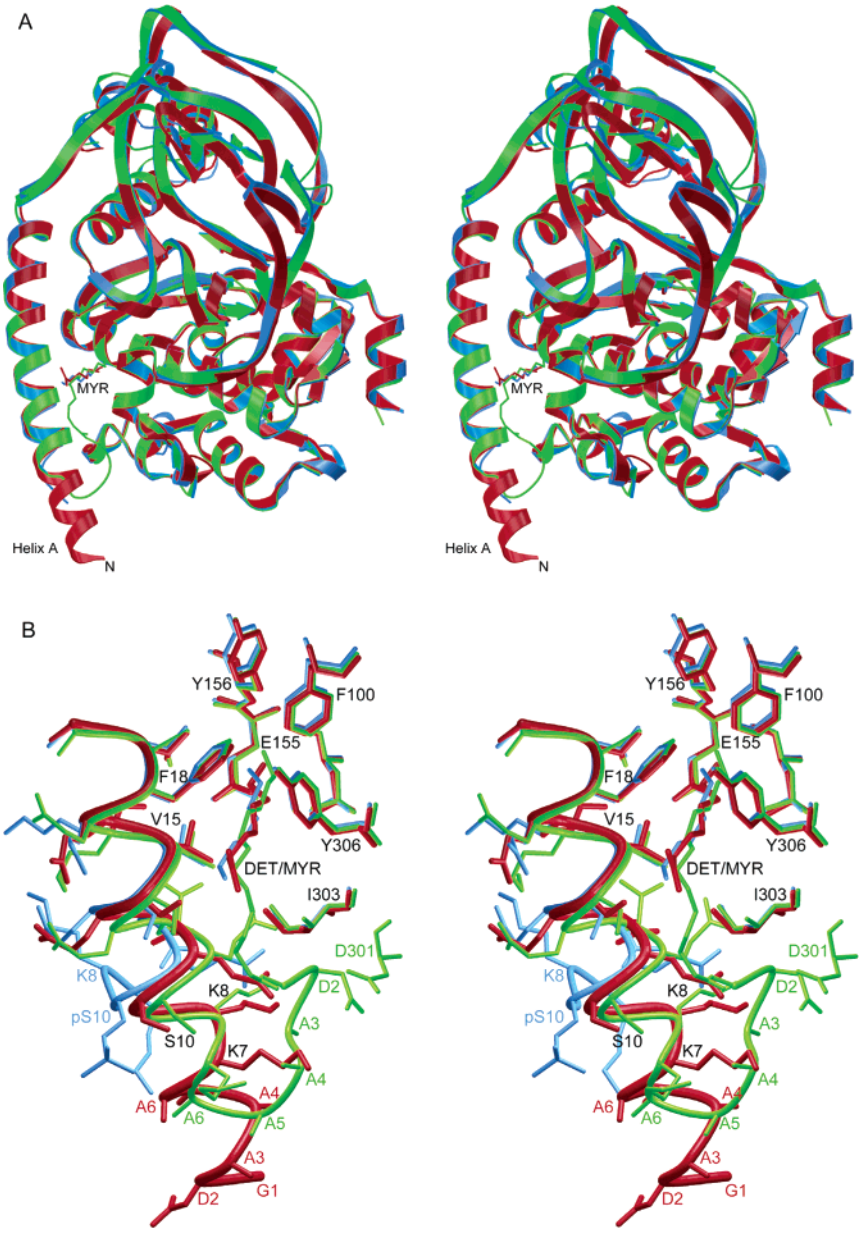

FIGURE 2: Overlay of three structures with different conformations of the N-terminus: 2-fold phosphorylated mutant PKAB4 (Thr197, Ser338) 2P-PKAB4 (red), 3-fold phosphorylated PKA (Ser10, Thr197, Ser338) 3P-PKA (1Q8U) (*39*) (blue), and 2-fold phosphorylated myristoylated PKA (Thr197, Ser338) 2P-myrPKA (1CMK) (*25*) (green) as representative of the myristoylated PKA structures. (A) Stereoview of the three structures. 2P-PKAB4 and 3P-PKA are in a closed conformation compared to the 2P-myrPKA structure. In 2P-PKAB4 and 3P-PKA, electron density at the myristate binding site has been interpreted as ordered parts of the MEGA-8, as previously described. (B) Details of the helical fold: In the 2P-PKAB4 structure, residues 1−31 form an ideal alpha helix, whereas the myristoylated structure 2P-myrPKA (1CMK) possesses a helix beginning at residue 6, apparently to allow the myristate to bind in its hydrophobic pocket. In contrast to both structures, the nonmyristoylated and Ser10 phosphorylated structure 3P-PKA (1Q8U), residues Gly9, Lys8, and Lys7 also form a turn, but in a direction distinct from 1CMK, and the remaining N-terminal residues are disordered.

Table 3: K_M Values of PKA and Mutants

	PKA	PKAB2	PKAB3	PKAB4
K_M ATP [μM]	12	128	30.6	141

neighboring Arg256). The new crystal packing could accommodate a phosphate group, at least spatially. As described in the results section, the N-terminus forms a salt bridge with Glu248.

On the basis of these considerations, and based on the destructuring effects of phosphorylation on N-terminal peptides (*12*), we propose that the lack of phosphorylation at Ser10 in unmyristoylated PKA stabilizes a completely helical form of the N-terminus, and conversely that phosphorylation at Ser10 enhances disorder of the 9 N-terminal residues. Since crystal structures of flexible proteins are typically "snapshots" of allowed configurations, the structure described here demonstrates the occurrence of the helical N-terminus form of the protein. Additionally, it corroborates the view that the lack of phosphorylation at Ser10 is associated with N-terminal helix formation.

Crystal structures and peptide experiments have identified N-terminal myristoylation, Asn2 deamidation, and Ser10 phosphorylation as potential modulators of structure (*12*). Myristoylation may prevent helical formation of the N-terminal residues of PKA to allow myristoyl binding to the

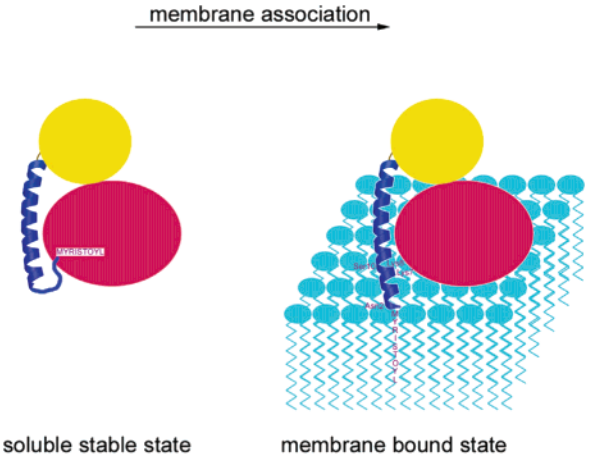

FIGURE 3: PKA in a soluble, stable state with myristate bound to a hydrophobic pocket in the C-terminal lobe (as in crystal structures 1CDK and 1CMK). In the membrane-associated form, the N-terminus can adopt its extended helical conformation (as in the structure reported here), thus exposing the myristoyl chain to the solvent and/or membrane. The basic side chains of Lys7 and Lys8, essential for membrane binding, are similarly extended and poised for membrane interactions. The posttranslational modification sites Ser10 (phosphorylation) and Asn2 (deamidation) that might modulate membrane binding properties (see text) are denoted in the figure.

hydrophobic pocket; however, it seems to increase helical structure in PKA N-terminal peptides. Ser10 phosphorylation is disordering in peptide experiments. Deamidated Asn2 is found in 30% of PKA isolated from muscle tissue (*14*). In peptide experiments (*12*), deamidation of Asn2 seems to be uncorrelated with structural changes, but may affect membrane binding affinity and has also been observed to influence the intracellular distribution of the kinase (*43*).

The observation of helix formation that projects the myristoylation position into the solution implies that the N-terminus is switchable between helical and myristoyl pocket bound states, and possibly other disordered states (Figure 3). In the absence of an alternative myristoyl binding position, the myristoyl chain binds in its endogenous pocket. In the absence of the myristoyl group and destructuring phosphorylation (at Ser10), the N-terminus adopts a helical fold as an extension of helix A. The geometry projects the myristoylation residue into solution.

The proximity of a myristoyl binding site as an alternative to the binding pocket of PKA would lower an energy penalty of vacating the pocket and push the equilibrium toward the extended helical state. Such potential binding interactions could be binding to a membrane or other protein domains.

PKA is bound to membranes in fibroblasts and can be released by platelet-derived growth factor (*22*). Further, association of N-terminal myristoylated peptides with phospholipids bicelles (*23*), binding of PKA-Src-chimerics to membranes (*21*) and interaction of myristoylated PKA with phosphatidylcholine/phosphatidylserine liposomes, synergistically in combination with the RII subunit (*24*), shows binding of myristoylated PKA to membranes using model systems. These and related phenomena should now be analyzed in light of a conformation of an extended helix A as can be seen in our structure.

The posttranslational modification positions at Asn2 and Ser10 are available to modulate transitions between membrane bound and unbound structures. One hypothetical scenario might begin with membrane association of myristoylated PKA with an extended helix geometry. Phosphorylation and/or deamidation introduces membrane repulsive negative charge and breaks the N-terminal helix structure (analogous to the phosphorylation modulation of Src membrane binding (*18*)). This dissociates PKA from the membrane, and the myristoyl residue is "parked" in the "storage pocket" while serine 10 is rapidly dephosphorylated (as shown in NMR experiments with alkaline phosphatase (*29*)).

ACKNOWLEDGMENT

We thank Lissy Weyher-Stingl for mass spectrometry.

REFERENCES

1. Engh, R. A., and Bossemeyer, D. (2001) The protein kinase activity modulation sites: Mechanisms for cellular regulation − Targets for therapeutic intervention. *Adv. Enzyme Regul. 41*, 121−149.
2. Engh, R. A., and Bossemeyer, D. (2002) Structural aspects of protein kinase control − role of conformational flexibility. *Pharmacol. Ther. 93*, 99−111.
3. Huse, M., and Kuriyan, J. (2002) The conformational plasticity of protein kinases. *Cell 109*, 275−282.
4. Scott, J. D. (1991) Cyclic nucleotide-dependent protein-kinases. *Pharmacol. Ther. 50*, 123−145.
5. Scott, J. D., and Carr, D. W. (1992) Subcellular-Localization of the Type-II cAMP-dependent protein-kinase. *News Physiol. Sci. 7*, 143−148.
6. Hubbard, M. J., and Cohen, P. (1993) On target with a new mechanism for the regulation of protein-phosphorylation. *Trends Biochem. Sci. 18*, 172−177.
7. Skalhegg, B. S., and Tasken, K. (2000) Specificity in the cAMP/PKA signaling pathway. Differential expression, regulation, and subcellular localization of subunits of PKA. *Frontiers Biosci. 5*, D678−D693.
8. Griffioen, G., and Thevelein, J. M. (2002) Molecular mechanisms controlling the localisation of protein kinase A. *Curr. Genet. 41*, 199−207.
9. Meinkoth, J. L., Ji, Y., Taylor, S. S., and Feramisco, J. R. (1990) Dynamics of the distribution of cyclic AMP-dependent protein-kinase in living cells. *Proc. Nat. Acad. Sci. U.S.A. 87*, 9595−9599.
10. Harootunian, A. T., Adams, S. R., Wen, W., Meinkoth, J. L., Taylor, S. S., and Tsien, R. Y. (1993) Movement of the free catalytic subunit of cAMP-dependent protein-kinase into and out of the nucleus can be explained by diffusion. *Mol. Biol. Cell 4*, 993−1002.
11. Wen, W., Meinkoth, J. L., Tsien, R. Y., and Taylor, S. S. (1995) Identification of a signal for rapid export of proteins from the nucleus. *Cell 82*, 463−473.
12. Tholey, A., Pipkorn, R., Bossemeyer, D., Kinzel, V., and Reed, J. (2001) Influence of myristoylation, phosphorylation, and deamidation on the structural behavior of the N-terminus of the catalytic subunit of cAMP-dependent protein kinase. *Biochemistry 40*, 225−231.
13. Yonemoto, W., McGlone, M. L., and Taylor, S. S. (1993) N-Myristylation of the Catalytic Subunit of cAMP-Dependent Protein-Kinase Conveys Structural Stability. *J. Biol. Chem. 268*, 2348−2352.
14. Jedrzejewski, P. T., Girod, A., Tholey, A., Konig, N., Thullner, S., Kinzel, V., and Bossemeyer, D. (1998) A conserved deamidation site at Asn 2 in the catalytic subunit of mammalian cAMP-dependent protein kinase detected by capillary LC-MS and tandem mass spectrometry. *Protein Sci. 7*, 457−469.
15. Tonerwebb, J., Vanpatten, S. M., Walsh, D. A., and Taylor, S. S. (1992) Autophosphorylation of the catalytic subunit of cAMP-dependent protein-kinase. *J. Biol. Chem. 267*, 25174−25180.
16. Yonemoto, W., McGlone, M. L., Grant, B., and Taylor, S. S. (1997) Autophosphorylation of the catalytic subunit of cAMP-dependent protein kinase in *Escherichia coli*. *Protein Eng. 10*, 915−925.
17. Johnson, D. A., Akamine, P., Radzio-Andzelm, E., Madhusudan, and Taylor, S. S. (2001) Dynamics of cAMP-dependent protein kinase. *Chem. Rev. 101*, 2243−2270.

18. Walker, F., Deblaquiere, J., and Burgess, A. W. (1993) Translocation of pp60(c-Src) from the plasma-membrane to the cytosol after stimulation by platelet-derived growth-factor. *J. Biol. Chem. 268*, 19552−19558.
19. McLaughlin, S., and Aderem, A. (1995) The myristoyl-electrostatic switch − a modulator of reversible protein-membrane interactions. *Trends Biochem. Sci. 20*, 272−276.
20. Hanakam, F., Albrecht, R., Eckerskorn, C., Matzner, M., and Gerisch, G. (1996) Myristoylated and non-myristoylated forms of the pH sensor protein hisactophilin II: Intracellular shuttling to plasma membrane and nucleus monitored in real time by a fusion with green fluorescent protein. *EMBO J. 15*, 2935−2943.
21. Silverman, L., and Resh, M. D. (1992) Lysine residues form an integral component of a novel NH2-terminal membrane targeting motif for myristylated pp60(v-Src). *J. Cell Biol. 119*, 415−425.
22. Deblaquiere, J., Walker, F., Michelangeli, V. P., Fabri, L., and Burgess, A. W. (1994) Platelet-derived growth-factor stimulates the release of protein-kinase-A from the cell-membrane. *J. Biol. Chem. 269*, 4812−4818.
23. Struppe, J., Komives, E. A., Taylor, S. S., and Vold, R. R. (1998) H-2 NMR studies of a myristoylated peptide in neutral and acidic phospholipid bicelles. *Biochemistry 37*, 15523−15527.
24. Gangal, M., Clifford, T., Deich, J., Cheng, X. D., Taylor, S. S., and Johnson, D. A. (1999) Mobilization of the A-kinase N-myristate through an isoform-specific intermolecular switch. *Proc. Natl. Acad. Sci. U.S.A. 96*, 12394−12399.
25. Zheng, J. H., Knighton, D. R., Xuong, N. H., Taylor, S. S., Sowadski, J. M., and Teneyck, L. F. (1993) Crystal-structures of the myristylated catalytic subunit of cAMP-dependent protein-kinase reveal open and closed conformations. *Protein Sci. 2*, 1559−1573.
26. Prade, L., Engh, R. A., Girod, A., Kinzel, V., Huber, R., and Bossemeyer, D. (1997) Staurosporine-induced conformational changes of cAMP-dependent protein kinase catalytic subunit explain inhibitory potential. *Structure 5*, 1627−1637.
27. Engh, R. A., Girod, A., Kinzel, V., Huber, R., and Bossemeyer, D. (1996) Crystal structures of catalytic subunit of cAMP-dependent protein kinase in complex with isoquinolinesulfonyl protein kinase inhibitors H7, H8, and H89 − Structural implications for selectivity. *J. Biol. Chem. 271*, 26157−26164.
28. Herberg, F. W., Bell, S. M., and Taylor, S. S. (1993) Expression of the catalytic subunit of cAMP-dependent protein-kinase in *Escherichia coli* − multiple isozymes reflect different phosphorylation states. *Protein Eng. 6*, 771−777.
29. Seifert, M. H. J., Breitenlechner, C. B., Bossemeyer, D., Huber, R., Holak, T. A., and Engh, R. A. (2002) Phosphorylation and flexibility of cyclic-AMP-dependent protein kinase (PKA) using P-31 NMR Spectroscopy. *Biochemistry 41*, 5968−5977.
30. Gassel, M., Breitenlechner, C. B., Ruger, P., Jucknischke, U., Schneider, T., Huber, R., Bossemeyer, D., and Engh, R. A. (2003) Mutants of protein kinase a that mimic the ATP-binding site of protein kinase B (AKT). *J. Mol. Biol. 329*, 1021−1034.
31. Olsen, S. R., and Uhler, M. D. (1989) Affinity purification of the C-alpha and C-beta isoforms of the catalytic subunit of cAMP-dependent protein-kinase. *J. Biol. Chem. 264*, 18662−18666.
32. Cook, P. F., Neville, M. E., Jr., Vrana, K. E., Hartl, F. T., and Roskoski, R., Jr. (1982) Adenosine cyclic 3′,5′-monophosphate dependent protein kinase: kinetic mechanism for the bovine skeletal muscle catalytic subunit. *Biochemistry 21*, 5794−5799.
33. Bailey, S. (1994) The CCP4 Suite − Programs for protein crystallography. *Acta Crystallogr., Sect. D: Biol. Crystallogr. 50*, 760−763.
34. Potterton, E., Briggs, P., Turkenburg, M., and Dodson, E. (2003) A graphical user interface to the CCP4 program suite. *Acta Crystallogr. Sect. D: Biol. Crystallogr. 59*, 1131−1137.
35. Gerber, P. R., and Muller, K. (1995) MAB, a generally applicable molecular-force field for structure modeling in medicinal chemistry. *J. Comput.-Aided Mol. Des. 9*, 251−268.
36. Kraulis, P. J. (1991) Molscript − a program to produce both detailed and schematic plots of protein structures. *J. Appl. Crystallogr. 24*, 946−950.
37. Esnouf, R. M. (1999) Further additions to MolScript version 1.4, including reading and contouring of electron-density maps. *Acta Crystallogr., Sect. D: Biol. Crystallogr. 55*, 938−940.
38. Merritt, E. A., and Bacon, D. J. (1997) Raster3D: Photorealistic molecular graphics. *Methods Enzymol. 277*, pp 505−524.
39. Breitenlechner, C., Gassel, M., Hidaka, H., Kinzel, V., Huber, R., Engh, R. A., and Bossemeyer, D. (2003) Protein kinase A in complex with rho-kinase inhibitors Y-27632, fasudil, and H-1152P: Structural basis of selectivity, *Structure 11*, 1595−1607.
40. Knighton, D. R., Bell, S. M., Zheng, J. H., Teneyck, L. F., Xuong, N. H., Taylor, S. S., and Sowadski, J. M. (1993) 2.0-Angstrom refined crystal-structure of the catalytic subunit of cAMP-dependent protein-kinase complexed with a peptide inhibitor and Detergent. *Acta Crystallogr. Sect. D: Biol. Crystallogr. 49*, 357−361.
41. Bossemeyer, D., Engh, R. A., Kinzel, V., Ponstingl, H., and Huber, R. (1993) Phosphotransferase and substrate binding mechanism of the cAMP-dependent protein-kinase catalytic subunit from porcine heart as deduced from the 2.0 angstrom structure of the complex with Mn2+ adenylyl imidodiphosphate and inhibitor peptide PKI(5−24). *EMBO J. 12*, 849−859.
42. Madhusudan, Akamine, P., Xuong, N. H., and Taylor, S. S. (2002) Crystal structure of a transition state mimic of the catalytic subunit of cAMP-dependent protein kinase. *Nat. Struct. Biol. 9*, 273−277.
43. Pepperkok, R., Hotz-Wagenblatt, A., König, N., Girod, A., Bossemeyer, D., and Kinzel, V. (2000) Intracellular distribution of mammalian protein kinase A catalytic subunit altered by conserved Asn2 deamidation. *J. Cell Biol. 148*, 715−726.

BI0362525